Eur. Phys. J. B **36**, 221–231 (2003)
DOI: 10.1140/epjb/e2003-00339-4

THE EUROPEAN PHYSICAL JOURNAL B

Spectral properties of the Brownian self-transport operator

D.S. Grebenkov[1,a], M. Filoche[1,2], and B. Sapoval[1,2]

[1] Laboratoire de Physique de la Matière Condensée, CNRS-École Polytechnique, 91128 Palaiseau, France
[2] Centre de Mathématiques et de leurs Applications, CNRS-École Normale Supérieure, 94140 Cachan, France

Received 17 June 2003
Published online 8 December 2003

Abstract. The problem of the Laplacian transfer across an irregular resistive interface (a membrane or an electrode) is investigated with use of the Brownian self-transport operator. This operator describes the transfer probability between two points of a surface, through Brownian motion in the medium neighbouring the surface. This operator governs the flux across a semi-permeable membrane as diffusing particles repetitively hit the surface until they are finally absorbed. In this paper, we first give a theoretical study of the properties of this operator for a planar membrane. It is found that the net effect of a decrease of the surface permeability is to induce a broadening of the region where a particle, first hitting the surface on one point, is finally absorbed. This result constitutes the first analytical justification of the *Land Surveyor Approximation*, a formerly developed method used to compute the overall impedance of a semi-permeable membrane. In a second step, we study numerically the properties of the Brownian self-transport operator for selected irregular shapes.

PACS. 41.20.Cv Laplace equation – 82.65.Jv Heterogeneous catalysis – 61.43.Hv Fractals

1 Introduction

Several transport phenomena in physics, chemistry and biology can be brought to a single mathematical frame: the transport across a "resistive" irregular surface driven by Laplacian fields. Examples can be found in electrochemistry (the Laplacian field is the electric field), in chemistry (steady state concentration gradients of chemical species in catalysis) or in physiology (steady state concentration gradients towards a semi-permeable membrane).

Let us consider the problem of steady-state bulk and membrane diffusion shown in Figure 1a. The concentration C of particles in the bulk is governed by the Laplace equation:

$$\Delta C = 0. \tag{1}$$

The flux in the bulk obeys Fick's law, $\mathbf{\Phi} = -D\nabla C$ where D is the diffusion coefficient. The flux across the surface is given by $\Phi_n = -WC$, where W is the membrane permeability (the probability per unit time, surface, and concentration for a particle to cross the membrane). Here the normal derivative is directed toward the bulk. The surface boundary condition obtained by equating both fluxes leads to a mixed boundary condition (often called Fourier or Robin boundary condition):

$$\frac{\partial C}{\partial n} = \frac{C}{\Lambda}, \qquad \text{with} \quad \Lambda = \frac{D}{W} \tag{2}$$

Finally, the concentration is supposed to be constant on a diffusion source far from the working membrane.

This problem is mathematically equivalent to a pure electrochemical problem in the same geometry: one considers an electrochemical cell with two electrodes, a planar and an irregular working electrode (with an interface resistivity r), placed in an electrolyte with a resistivity ρ (Fig. 1b). In this case, the electric potential V obeys the Laplace equation (1), the quantity $1/\rho$ plays the role of the diffusion coefficient D, and $1/r$ corresponds to the permeability W. The same mixed boundary condition as in (2) appears with $\Lambda = r/\rho$ (see [2–4])[1]. The same correspondence exists between the diffusion problem and heterogeneous catalysis on an irregular surface. Consequently, one can restrict to the diffusion problem and eventually apply the results to other problems.

After a brief recall on the theoretical introduction of the Brownian self-transport operator (or BSO) [3], we discuss

– the spectral properties of this operator as these properties govern the diffusive transfer across the interface. This will be done analytically and checked by simulations for a planar membrane;

[a] e-mail: denis.grebenkov@polytechnique.fr

[1] In the framework of the impedance spectroscopy, the interface resistivity r should be replaced by the specific surface impedance $1/(-i\gamma\omega)$, where ω is the frequency and γ is the capacitance per unit area. It implies that Λ is inversely proportional to ω.

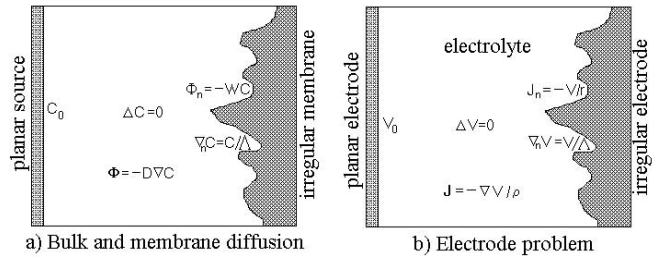

Fig. 1. The problem of the Laplacian transfer across a resistive irregular interface (a membrane or an electrode).

– the response of a few typical irregular shapes (first generations of a fractal surface, a deep pore, etc.) based on the numerical study of the properties of the Brownian self-transport operator;
– how this formalism gives a detailed analytical and numerical justifications for the *Land Surveyor Approximation*. It will be found that the parameter Λ really plays the role of an approximate *absorption perimeter*.

2 The Brownian self-transport operator (BSO)

We briefly recall the BSO formalism introduced in [3]. The physical ideas underlying this approach were first brought forward by Halsey [11]. Although this formalism applies in any space dimension, we focus ourselves in this paper to the two-dimensional case ($d = 2$), in order to compare theoretical results and accurate numerical simulations.

In the diffusion case, particles start from a distant source and walk at random on a square lattice with lattice parameter a and hopping rate τ^{-1} until they hit a semi-permeable membrane of perimeter L_p, discretized into N sites, with $L_p = Na$. Each time a particle arrives on a site of the membrane, it may be absorbed, with a probability σ. The semi-permeable membrane is thus characterized by a *reflection probability* $\varepsilon = 1 - \sigma$.

It has been shown [3] that the macroscopic response of such a system can be fully computed by mean of two sets of quantities:

– the probabilities $(P_{0,j})_{1\leq j\leq N}$ for a random walk starting on the distant source to land *at first hit* on the site j of the membrane. These numbers define a vector $\mathbf{P_0}$ that represents the distribution of first arrivals on the membrane;
– the probabilities $(Q_{jk})_{1\leq j,k\leq N}$ for a random walk starting on a site j of the membrane to land *at first hit* on the site k of the membrane. These probabilities (Q_{jk}) define a linear operator, the *Brownian self-transport operator* Q, that transforms a distribution on the membrane into another distribution on the same membrane. This operator depends only on the geometry of the system.

Note that these distributions of hitting probabilities depend on the discretization: all discrete quantities defined with the help of $\mathbf{P_0}$ and Q, depend on a. Only in the continuous limit $a \to 0$, this dependence is suppressed. We will briefly discuss the continuous limit at the end of the paper, Section 4.2. From now on, a is considered as a fixed parameter.

In the case of a perfectly absorbing surface ($\varepsilon = 0$), the random walkers are absorbed at first hit, and $\mathbf{P_0}$ represents the current distribution crossing the membrane. Introducing a positive reflection probability ε induces a modification of this current distribution, as particles have to bounce again and again on the membrane before being absorbed. The modified current distribution, called $\mathbf{P}_\varepsilon$, is deduced from $\mathbf{P_0}$ through a *spreading operator* T_ε that depends on Q and ε: $\mathbf{P}_\varepsilon = T_\varepsilon\, \mathbf{P_0}$, with:

$$T_\varepsilon = \sum_{n=0}^{\infty} (1-\varepsilon)\, \varepsilon^n\, Q^n = (1-\varepsilon)(I-\varepsilon Q)^{-1} \qquad (3)$$

where I stands for the identity operator. This relation expresses that the distribution $\mathbf{P}_\varepsilon$ is obtained by summing the hitting probabilities over all possible number of hits against the membrane. It is useful to note that this operator can be expressed in the following form:

$$T_\varepsilon = \left[\, I + \Lambda \left(\frac{I-Q}{a}\right) \,\right]^{-1} \quad \text{with} \quad \Lambda = a\, \frac{\varepsilon}{1-\varepsilon}. \quad (4)$$

This parameter Λ, as shown below, corresponds, in the continuous limit, to $\Lambda = D/W$ introduced in (2).

Using a vectorial formalism, the spectroscopic impedance of the membrane can be expressed as a scalar product between two normalized distributions $\mathbf{P}^{\mathbf{h}}_\varepsilon$ and $\mathbf{P^h_0}$ (in the continuous limit, $\mathbf{P^h_0}$ corresponds to the *harmonic measure* of the membrane for a source at infinite distance):

$$Z(\varepsilon) = \frac{4\tau\varepsilon}{1-\varepsilon}\ \left(\mathbf{P}^{\mathbf{h}}_\varepsilon \cdot \mathbf{P^h_0}\right) \qquad (5)$$

in which the following normalization procedure has been used:

$$\mathbf{P}^{\mathbf{h}}_\varepsilon = \frac{\mathbf{P}_\varepsilon}{a(\mathbf{P}_\varepsilon \cdot \mathbf{1})}, \quad \mathbf{1} = (1,1,...,1).$$

Finally, the scalar product can be developed on the eigenvectors $\mathbf{V}_\alpha$ of the operator Q (with eigenvalues q_α), which leads to the following expression for $Z(\varepsilon)$ [2]:

$$Z(\varepsilon) = \left(\frac{4\tau\varepsilon}{1-\varepsilon}\right) \sum_\alpha \frac{\left(\mathbf{P^h_0} \cdot \mathbf{V}_\alpha\right)^2}{1+\Lambda\left(\dfrac{1-q_\alpha}{a}\right)}. \qquad (6)$$

One sees that the geometry of the membrane governs the transfer properties *only through the spectral properties*

[2] The spectroscopic impedance is given by this relation in the limit when the source goes to infinity. For finite distances between the source and the membrane, one has [3]:

$$Z_{finite}(\varepsilon) = \frac{1}{Z(\varepsilon)^{-1} - R_0^{-1}} \quad \text{with} \quad R_0 = \frac{1}{D(\mathbf{P_0} \cdot \mathbf{1})}$$

R_0 is the bulk access impedance of the cell.

of the operator Q. One introduces the density of states $\mathcal{D}_a(q)$ and the relative weight of each eigenmode $C_a^2(q_\alpha)$:

$$\mathcal{D}_a(q) = \frac{1}{N}\sum_\alpha \delta(q-q_\alpha), \quad C_a^2(q_\alpha) = N\, a\, \left(\mathbf{P_0^h}\cdot\mathbf{V}_\alpha\right)^2.$$

It will be shown in the next section that the density of states $\mathcal{D}_a(q)$ is only weakly dependent on the membrane geometry so that the Laplacian transfer is mainly determined by the weighting function $C_a(q)$. Furthermore, the factor $\Lambda\left(\frac{1-q}{a}\right)$, that appears in the denominator, suggests that one should especially examine the behavior of the eigenvalues and eigenvectors around $q_\alpha = 1$ in the usual case where $\Lambda \gg a$ (or when $a \to 0$).

In order to express the results in terms of the real physical parameters describing the continuous problem, we recall how the transport parameters of the model are related to the lattice (discrete) parameters (a, τ, ε) [3]. First, the diffusion coefficient for a square lattice in two dimensions ($d = 2$) is:

$$D = \frac{a^2}{2d\tau} = \frac{a^2}{4\tau}.$$

The membrane permeability W depends on the reflection probability ε (see Appendix):

$$W = \frac{a}{2d\tau}\frac{1-\varepsilon}{\varepsilon} = \frac{a}{4\tau}\frac{1-\varepsilon}{\varepsilon}.$$

The length $\Lambda = D/W$ defined in (2) can thus be written as:

$$\Lambda = a\,\frac{\varepsilon}{1-\varepsilon}. \tag{7}$$

Before proceeding, it is useful to recall the known spectral properties of the BSO [3,9]:

- Eigenvalues (q_α) lie on the interval $[-1, 1]$.
- There always exists a maximal eigenvalue q_{max} exceeding the other ones; the coordinates of corresponding eigenvector $\mathbf{V}(q_{max})$ are positive (Perron-Frobenius theorem). If the source goes to infinity, $q_{max} \to 1$ and $\mathbf{V}(q_{max}) \to (1/\sqrt{N})\,\mathbf{1}$. Moreover, $q_{max} \approx 1$ for a reasonable distance between the source and the membrane.
- The other eigenvectors are orthogonal to $\mathbf{V}_{max}$, thus one has $(\mathbf{V}_\alpha \cdot \mathbf{1}) = \sum_i (\mathbf{V}_\alpha)_i \to 0$ when the source goes to infinity.

In the following section, one will show that it is possible to draw exact results for the spectral properties of Q in the case of a planar membrane. These results will then help to understand the general case of a geometrical irregularity.

3 Eigenvalues and eigenvectors of Q

3.1 The planar membrane

3.1.1 Eigenvalues

We consider a *finite* planar membrane with periodic (cyclic) boundary conditions. Such membrane can be regarded as a boundary of a cylinder, i.e., a circle. In this case, the matrix Q is cyclic ($Q_{i,j} = Q_{0,j-i}$) and its eigenvectors $(\mathbf{V}_\alpha)_{0\le\alpha<N}$ are simply the associated Bloch vectors (one defines $Q_{0,-n} = Q_{0,n}$):

$$q_\alpha = \sum_{n=-\frac{N}{2}}^{\frac{N}{2}-1} Q_{0,n}\, e^{-ik_\alpha n a} \tag{8}$$

$$\mathbf{V}_\alpha = \frac{1}{\sqrt{N}}\, e^{ik_\alpha \boldsymbol{r}} \tag{9}$$

with: $\quad k_\alpha = \dfrac{2\pi\alpha}{Na} = \dfrac{2\pi\alpha}{L}$ and $\boldsymbol{r} = \begin{pmatrix} a \\ 2a \\ \dots \\ Na \end{pmatrix}$.

These vectors represent discrete sine-waves with spatial frequency k_α. It is clear that almost all the eigenvalues are doubly degenerated (except q_0 and $q_{\frac{N}{2}}$) since:

$$q_{N-\alpha} = q_\alpha. \tag{10}$$

To go further, we need some informations about the elements of the matrix Q. According to the definition (see Sect. 2), $Q_{i,j}$ is the probability that a random walker starting from the point i (of coordinates $(a\times i, 0)$) will hit the membrane at point j (of coordinates$(a\times j, 0)$) at the first contact. This distribution admits an exact analytical expression [7,10]:

$$Q_{0,n} = \frac{1}{N}\sum_{\alpha=-\frac{N}{2}}^{\frac{N}{2}-1} e^{ik_\alpha n a}\ \varphi(k_\alpha a) \tag{11}$$

where: $\varphi(x) = \left(\sqrt{1+\sin^2(x/2)} - |\sin(x/2)|\right)^2$.

Using equations (11) and (8), one immediately deduces the eigenvalues:

$$q_\alpha = \left(\sqrt{1+\sin^2\left(\frac{k_\alpha a}{2}\right)} - \left|\sin\left(\frac{k_\alpha a}{2}\right)\right|\right)^2. \tag{12}$$

As the function $\varphi(x)$ decreases on the interval $[0, \pi]$, one has a decreasing sequence of eigenvalues q_α. In the same time, the spatial frequencies k_α are increasing. It means that eigenvectors of larger eigenvalues correspond to slower spatial frequencies. Finally, inverting equation (12) gives the spatial frequency of each mode as a function of its eigenvalue:

$$k(q) = \frac{2}{a}\arcsin\left(\frac{1-q}{2\sqrt{q}}\right). \tag{13}$$

One should note that, around $q = 1$: $\quad k(q) \approx \left(\dfrac{1-q}{a}\right)$.

The eigenvectors of the BSO behave as oscillating functions, and they form a complete basis. Therefore these vectors can be viewed as a pseudo-Fourier basis generated by the surface geometry. In the case of a planar membrane,

one deals with a properly Fourier basis (see Eq. (9)). Moreover, the ordering of eigenvalues provides the means to control the spatial frequencies of these vectors. We have demonstrated for a planar membrane, and we will see by numerical simulations for other geometries, that low frequency vectors correspond to eigenvalues in the vicinity of 1, and vice-versa. In this light, $C_a(q_\alpha)$ are the coefficients of the pseudo-Fourier decomposition of the harmonic measure.

3.1.2 Density of states

The eigenvalues $\{q_\alpha\}$ calculated in the previous section, in the limit of a very large number of sites ($N \to \infty$), are distributed according an *integrated density of states* $\mathcal{N}_2(q)$ (the 2 here stands for the embedding dimension) for the planar membrane:

$$\mathcal{N}_2(q) = \frac{2}{\pi} \arccos\left(\frac{1-q}{2\sqrt{q}}\right). \tag{14}$$

Taking the derivative, one writes the *differential density of states* $\mathcal{D}_2(q) = d\mathcal{N}_2(q)/dq$:

$$\mathcal{D}_2(q) = \frac{1}{\pi} \frac{1+q}{q\sqrt{q_m - q}} \frac{1}{\sqrt{q - q_0}} \tag{15}$$

where $q_0 = 3 - \sqrt{8}$, $q_m = 3 + \sqrt{8}$.

As explained earlier in this paper, the values $q \approx 1$ are of particular interest since they provide the largest contributions to the impedance. One can see here both the integrated and differential densities of states do not present any singularity around $q = 1$. This statement remains valid for different geometries as shown numerically in the next subsection.

3.1.3 Spectroscopic impedance

As the membrane and the source are planar, $\mathbf{P_0^h} = (L_p^{-1})\mathbf{1}$ (the harmonic measure is uniform). Thus, its scalar product with any eigenvector $\mathbf{V}_\alpha$ is equal to 0 except for $\alpha = 0$, for which it gives N/L_p^2. Only this mode contributes to the spectroscopic impedance, leading to the classical value:

$$Z(\Lambda) = \frac{\Lambda}{DL_p} = \frac{1}{WL_p}. \tag{16}$$

3.2 Irregular geometries

We now compare the behavior of the planar geometry with results obtained by numerical simulations for self-similar surfaces (Fig. 2a) and deep pores (Fig. 2b). Two different numerical tools were used: a discrete boundary integral method and Monte Carlo simulations of the diffusion process, with the same results. These numerical simulations show that the integrated density of states of a flat membrane, $\mathcal{N}_2(q)$, is a good approximation of the integrated densities of states of other membrane geometries

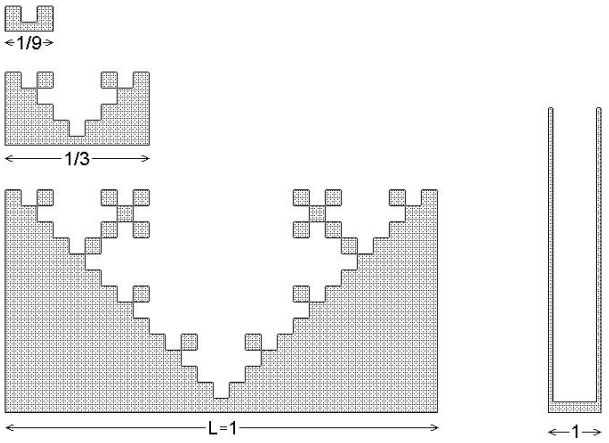

Fig. 2. Simple membrane shapes to study the spectral properties of the Brownian self-transport operator. Left: three generations of the fractal membrane with Hausdorff dimension $D_f = \ln 5/\ln 3 \approx 1.465$. The width L of the third generation is chosen equal to 1 (this is the unit of length). Each linear segment is represented by 10 points, i.e., the generation g is discretized into $N = 10 \times 5^g$ points. The lattice parameter is then $a = L_p/N = 3^{-3}/10 \approx 3.7 \times 10^{-3}$ since $L_p = (5/3)^3$ for the third generation. Right: The deep pore of width $L = 1$ and of depth 8.

(see Fig. 3). The latter exhibit the form of $\mathcal{N}_2(q)$ with only small variations. Thus, the integrated density of states is essentially independent on the geometry. The transfer across irregular membranes is then essentially determined by the spatial dependency of the eigenvectors of Q (more precisely, their scalar product with the normalized first arrival distribution $\mathbf{P_0^h}$ (or harmonic measure)).

One can draw a qualitative explanation for this fact. The random walker originated from a site of the membrane will be absorbed with high probability near its starting point. In mathematical terms, the operator Q is diagonal dominant (the elements of Q closer to the matrix diagonal are larger than the other matrix elements). As each membrane is locally planar, these elements almost do not depend on the membrane geometry. So, the membrane geometry mainly modifies the values of the matrix elements far from the diagonal. As a consequence, the eigenvalues, which are determined essentially by the dominating elements, depend weakly on the geometry. On the other hand, the eigenvectors are determined by the entire structure of the matrix Q.

3.2.1 A pre-fractal geometry

Numerical computations of the spectral properties of the BSO allow to study the function $C_a^2(q)\mathcal{D}_a(q)$ for various geometries. According to (6), this function essentially determines the spectroscopic impedance. Figure 4 displays this function for the third generation of the fractal membrane shown in Figure 2a for different distances h between the source and the membrane. One can distinguish three features:

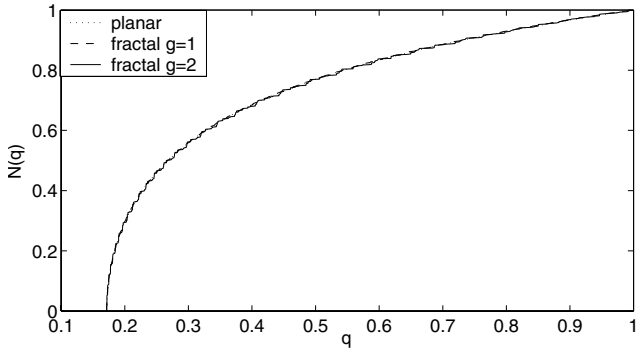

Fig. 3. Integrated densities of states $\mathcal{N}(q)$ calculated for the first and second generations of the fractal membrane of Figure 2a are very close to the function $\mathcal{N}_2(q)$ for the planar case.

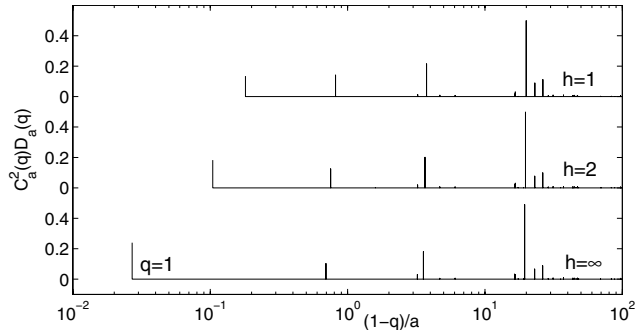

Fig. 4. The discrete geometrical spectrum $C_a^2(q)\mathcal{D}_a(q)$ for the third generation of the fractal membrane of Figure 2a for different distances h between the source and the membrane. The first peak q_0 goes to 1 when $h \to \infty$ while the other peaks do almost not depend on h.

– the largest eigenvalue q_{max} will tend to 1 as the source goes to infinity. This corresponds to a contribution Λ/DL_p which is the asymptotic behavior of the membrane impedance for large Λ:

$$\left(\mathbf{P_0^h} \cdot \mathbf{V}(q_{max})\right)^2 \approx \frac{1}{Na^2}$$

– the following several peaks come from the pre-fractal geometry of the membrane. The locations of the peaks are almost independent of the distance from the source;
– only a *very small number* of peaks significantly contribute to the spectroscopic impedance.

In order to understand the origin of the principal peaks, we have compared three pre-fractal membranes of increasing generation (Fig. 2a). Figure 5 shows that $(g-1)$ principal peaks of gth generation are almost identical to the peaks of the previous generations. For example, the second and third peaks of the third generation coincide with two peaks of the second generation. This result can be qualitatively explained by the following: the gth generation of the fractal membrane is composed of 5 "blocks", each of them being the $(g-1)$th generation of the same membrane. We discussed earlier that the probability for the random walker to go far from the starting point is small. In particular, the overwhelming majority of random

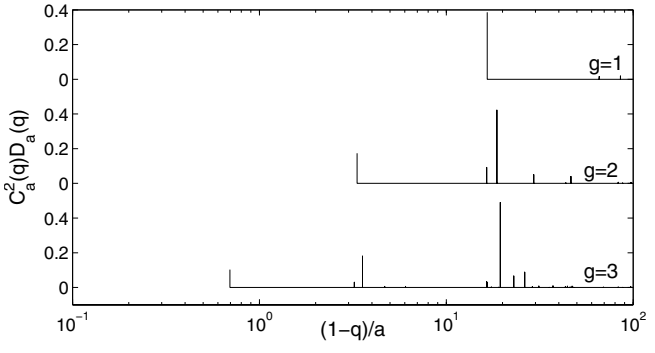

Fig. 5. The discrete geometrical spectrum $C_a^2(q)\mathcal{D}_a(q)$ for first three generations of the fractal membrane of Figure 2a, for a source at infinite distance. The last spectrum corresponds to the last spectrum in Figure 4 (the peak $q_0 = 1$ is not represented).

walks remains in each "block" of the membrane. Physically, this can be viewed as a relatively small interaction between these blocks. Then the first approximation

$$Q^{(g)} \approx \begin{pmatrix} Q^{(g-1)} & 0 & 0 & 0 & 0 \\ 0 & Q^{(g-1)} & 0 & 0 & 0 \\ 0 & 0 & Q^{(g-1)} & 0 & 0 \\ 0 & 0 & 0 & Q^{(g-1)} & 0 \\ 0 & 0 & 0 & 0 & Q^{(g-1)} \end{pmatrix} \quad (17)$$

allows to relate the eigenvalues and eigenvectors of the matrices $Q^{(g)}$ and $Q^{(g-1)}$ and explains the coincidence of $(g-1)$ principal peaks between both generations. Note that a good agreement between the numerical simulations and this theoretical explanation is provided by the fact that the first approximation (17) is relatively accurate. Such approximation formally leads to a spectrum degeneracy: any eigenvalue of matrix $Q^{(g)}$ becomes at least five times degenerate. However, among the five corresponding eigenvectors only one gives a significant contribution to the spectroscopic impedance once being projected onto harmonic measure. The positions of the peaks can also be interpreted. For example, the principal peak that corresponds to the highest value of q (after 1) is almost at the same position for the three pre-fractal structures: $(1-q)/a \approx 20$, in the three spectra, see Figure 5. This quantity gives a spatial frequency $k(q) \approx (1-q)/a \approx 20$, or equivalently, a typical wavelength of order 0.3. It corresponds to an eigenmode of the Brownian self-transport operator that varies on a length which is the *typical* perimeter of the smallest pre-fractal geometry ($(5/3)\cdot(L/9)$, upper geometry in Fig. 2a). At each generation, a new contributing peak appears, whose corresponding spatial frequency is approximately 5 times smaller. This corresponds to a typical length 5 times larger, which is the homothety ratio of the perimeter of the new geometry.

Interestingly, deterministic pre-fractal membranes only exhibit a small number of contributing peaks. The scale invariance of the fractal geometry yields an analogous hierarchical structure of the BSO and, by consequence, of its eigenvectors. The Q-eigenvectors whose spatial wavelength is substantially smaller than the typical

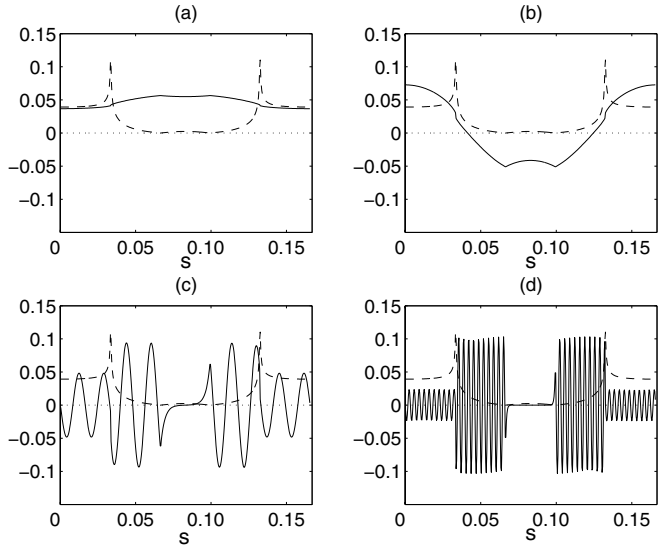

Fig. 6. Several eigenvectors $\mathbf{V}_\alpha$ of matrix Q (solid lines) and harmonic measure $\mathbf{P_0^h}$ (dashed lines; all values of $\mathbf{P_0^h}$ are multiplied by $10a$ in order to be comparable with eigenvectors) for the first generation of the fractal membrane of Figure 2a: (a) The eigenvector with all positive components for $\alpha = 0$ corresponds to the highest eigenvalue, $(1 - q_0)/a = 3.1$ (this value is not equal to 0 as the source is placed at finite distance from the membrane); (b) Next smooth eigenvector with $\alpha = 1$, $(1-q_1)/a = 21.5$; (c) Eigenvector with $\alpha = 20$ oscillates slowly, $(1-q_{20})/a = 321.2$; (d) High-frequency eigenvector with $\alpha = 100$, $(1 - q_{100})/a = 1194.1$. Here s is the curvilinear coordinate along the membrane surface, $L = 1/9$, $L_p = 5/27$. In order to obtain these figures in high resolution, we took the first generation with 90 points per segment, i.e., $N = 5 \times 90$ and $a = L_p/N = 4.1152 \times 10^{-4}$. Note that quantities $(1-q_\alpha)/a$ are almost independ of a discretization.

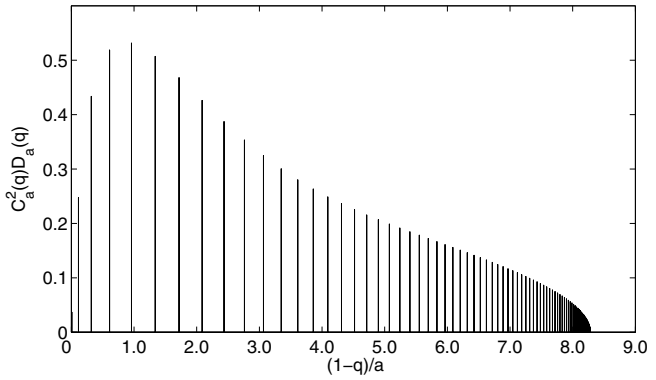

Fig. 7. The discrete geometrical spectrum $C_a^2(q)\mathcal{D}_a(q)$ for the deep pore in Figure 2b.

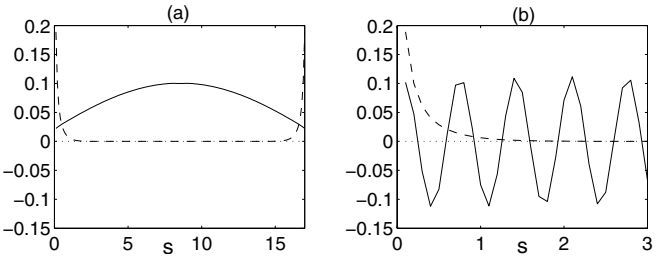

Fig. 8. Two eigenvectors $\mathbf{V}_\alpha$ of matrix Q (solid lines) and harmonic measure $\mathbf{P_0^h}$ (dashed lines; all values of $\mathbf{P_0^h}$ are multiplied by $10a$ in order to be comparable with eigenvectors) for the deep pore membrane: (a) The eigenvector with all positive components for $\alpha = 0$ corresponds to the highest eigenvalue $q_0 = 0.99875$; (b) High-frequency eigenvector with $\alpha = 50$, $q_{50} = 0.41669$ (first several periods). Here s is the curvilinear coordinate along the membrane surface, $L = 1$, $L_p = 17$, $a = 0.1$.

features of the geometry, bear a very small contribution as their scalar products with the harmonic measure $\mathbf{P_0^h}$ are practically negligible. This can be easily understood as these modes oscillate rapidly while the harmonic measure varies slowly compared to their frequency (Fig. 6).

3.2.2 Deep pores

Figure 7 displays the product $C_a^2(q)\mathcal{D}_a(q)$ for the deep pore in Figure 2b. Comparing with the fractal case, this function exhibits a significant difference. In the case of a deep pore, all eigenmodes contribute as shown in Figure 8. The harmonic measure on the deep pore is localized at the pore entrance on a small part of the surface. Therefore, many eigenmodes have a contribution to the spectroscopic impedance if they oscillates with a not too large spatial frequency as compared to the spatial extent of the harmonic measure.

Such differences in the behavior of the scalar products of the harmonic measure with oscillating eigenvectors of the BSO strongly influence the behavior of the spectroscopic impedance with respect to the physical parameters (ε or Λ). For example, as predicted by theoretical approaches [11–13], the spectroscopic impedance of self-similar electrodes should exhibit a power law response $Z(\Lambda) \sim \Lambda^\beta$ with $\beta = \tau(2)/D_f$ (in two dimensions). Here $\tau(2)$ is the correlation dimension of the harmonic measure and D_f is the Hausdorff dimension of the surface. In contrast, the deep pore impedance behaves as $Z(\Lambda) \sim \Lambda^\beta$ with $\beta = 0.5$.

4 The spreading operator

The Brownian self-transport operator, studied in the previous section, represents the probabilities for a particle to go through random walk from one site to another site of the membrane without touching the membrane in between. From its spectral properties, one can understand the properties of the spreading operator T_ε that determine the distribution $\mathbf{P}_\varepsilon$ of the absorbed random walkers on the membrane.

Up to now, the number N of sites on the membrane was an arbitrary finite parameter. In the first subsection, one examines the properties of the spreading operator in the planar case, the lattice parameter a being a fixed length. In the following subsections, one studies the *continuous* limit: $N \to \infty$, $a \to 0$, the perimeter of the membrane $L_p = Na$ being fixed.

4.1 The discrete planar membrane

In the limit $N \to \infty$, the probability $Q_{0,n}$ for any given n takes the following expression (using (11)):

$$Q_{0,n} = \int_0^\pi \frac{d\theta}{\pi} \cos(n\theta)\ \varphi(\theta). \tag{18}$$

By definition, $Q_{0,n}$ is the distribution of hitting probabilities on the integer horizontal axis when random walks are originated from the point of coordinates $(0,0)$. For large n, the asymptotic behavior of this probability can be derived (by integrating by part four times):

$$Q_{0,n} = \frac{1}{\pi n^2} - \frac{1}{2\pi n^4} + O(n^{-6}). \tag{19}$$

The spreading operator

$$T_\varepsilon = (1-\varepsilon)(I - \varepsilon Q)^{-1}$$

that transforms the first arrival distribution $\mathbf{P_0}$ (proportional to the harmonic measure) into the real absorption distribution $\mathbf{P}_\varepsilon$, can be conveniently represented for the planar membrane. In this case, T_ε has the same cyclic structure as Q, i.e., $(T_\varepsilon)_{i,j} = (T_\varepsilon)_{0,j-i}$. A direct calculation yields:

$$(T_\varepsilon)_{0,n} = (1-\varepsilon) \int_0^\pi \frac{d\theta}{\pi} \frac{\cos(n\theta)}{1-\varepsilon\varphi(\theta)}. \tag{20}$$

Again, an asymptotic behavior of $(T_\varepsilon)_{0,n}$ for large n can be derived from (20):

$$(T_\varepsilon)_{0,n} = \frac{1}{\pi n^2}\frac{\varepsilon}{1-\varepsilon} - \frac{1}{2\pi n^4}\frac{\varepsilon(\varepsilon^2+10\varepsilon+1)}{(1-\varepsilon)^3} + O(n^{-6}). \tag{21}$$

This important result shows that the spreading operator T_ε has, in general, a behavior similar to that of the initial operator Q. Comparing the leading terms of the asymptotics (19) and (21) of $Q_{0,n}$ and $(T_\varepsilon)_{0,n}$, one obtains for large n that

$$(T_\varepsilon)_{0,n} \gg Q_{0,n} \quad \text{for } \Lambda \gg a \text{ and } n \gg 1.$$

We mentioned above that the usual case is $\Lambda \gg a$, i.e., ε is near 1. In this case, the asymptotic behavior of elements $(T_\varepsilon)_{0,n}$ for fixed n can be computed in the limit $\varepsilon \to 1$ (or $\sigma \to 0$, where $\sigma = 1-\varepsilon$ is the *absorption probability*):

$$(T_\varepsilon)_{0,n} \sim -\sigma \ln \sigma. \tag{22}$$

This relation shows that the elements of $(I-\varepsilon Q)^{-1}$ tend to infinity logarithmically, but the $(T_\varepsilon)_{0,n}$ themselves tend to 0 just as required.

4.2 The continuous limit

Up to now, we have studied finite operators to address the discrete problem of the Laplacian transfer across an interface. It is interesting to see how the spectral properties of these operators behave in the limit of the continuous problem and how this knowledge can help to solve the mixed boundary problem defined by (1) and (2).

4.2.1 The continuous BSO

In the continuous limit, random walks are replaced by Brownian motions. In that frame, it is no more possible to define the probability density to go from one location of the membrane to another. One has to use for the origin of the Brownian motion a point located slightly above the membrane (which is the horizontal axis Oy in the planar case). The probability distribution of first hit on the horizontal axis for a two-dimensional Brownian motion starting at point (x,y) above the horizontal axis is given by a Cauchy density [5]:

$$\omega_0^{(y)}(x,x') \ = \ \frac{1}{\pi}\ \frac{y}{y^2+(x-x')^2}. \tag{23}$$

This expression is the continuous analog of the element $Q_{i,j}$ of the discrete operator. Yet, it depends on a real parameter y and converges towards a Dirac distribution $\delta(x-x')$ when y goes to 0:

$$\lim_{y\to 0}\ \omega_0^{(y)}(x,x') \ = \ \delta(x-x').$$

Thus, the continuous Brownian self-transport operator $Q^{(y)}$ defined by its kernel $\omega_0^{(y)}$ converges towards the identity when $y \to 0$. Nevertheless, one will see in the next subsection that the continuous spreading operator defined from this BSO converges to a non-trivial operator when $y \to 0$.

Note: The Cauchy distribution in (23) is frequently used as an approximation for the discrete case (18), although it has been shown that this approximation is not sufficient to accurately evaluate the spectral properties of the BSO [9]. For example, if one compares the asymptotics of the discrete (19) and the continuous (23) probabilities, one can see that their first terms (order n^{-2}) are identical but that the coefficients of the second terms (n^{-4}) are different ($1/2\pi$ versus $1/\pi$).

4.2.2 The continuous spreading operator

The discrete model involves three *independent* parameters: a, τ and ε. In the continuous limit of the discrete formalism, the lattice disappears, which corresponds to take $a \to 0$, the macroscopic transport parameters being kept constant. It then implies:

$$\tau = \frac{a^2}{4D} \to 0, \quad \varepsilon = \left(1+\frac{a}{\Lambda}\right)^{-1} \to 1, \quad N = \frac{L_p}{a} \to \infty.$$

In this limit, there are only two independent parameters: D and Λ (or D and W). The random walks with reflections on the membrane in the continuous limit become the *partially reflecting Brownian motion*.

From the continuous BSO $Q^{(y)}$ defined in the previous section, one can derive a continuous spreading operator $T_\Lambda^{(y)}$:

$$T_\Lambda^{(y)} \ = \ \left[\ I + \Lambda\ \left(\frac{I-Q^{(y)}}{y}\right)\ \right]^{-1}. \tag{24}$$

This continuous spreading operator can be calculated in several different ways. It can be deduced as a limit of the discrete spreading operator $(T_\varepsilon)_{0,n}$ for the planar membrane when $a \to 0$. The calculation steps are:

- replace the discrete index n by continuous coordinate $x = na$ and take $y = a$;
- sum the values of $(T_\varepsilon)_{0,n}$ lying on the interval $(x, x + \Delta x)$ with $\Delta x \gg a$;
- take the limit $a \to 0$.

Executing carefully these operations, one finally obtains an integral operator T_Λ, defined by its kernel t_Λ, that transforms a distribution $u(x)$ on the interface into another distribution $v(x)$ on the interface such that:

$$v(x) \;=\; T_\Lambda[u](x) \;=\; \int_{-\infty}^{\infty} t_\Lambda(x - x')\; u(x')\; dx'$$

$$\text{with} \qquad t_\Lambda(x) = \frac{1}{\pi} \int_0^{\infty} \cos(kx)\; \frac{dk}{1 + k\Lambda}. \qquad (25)$$

This integral can also be represented in terms of special functions:

$$t_\Lambda(x) = -\frac{1}{\pi\Lambda}\left[si\left(\frac{x}{\Lambda}\right)\sin\left(\frac{x}{\Lambda}\right) + ci\left(\frac{x}{\Lambda}\right)\cos\left(\frac{x}{\Lambda}\right)\right]$$

where $si(x)$ and $ci(x)$ are the integral sine and integral cosine functions [6]. By definition, $t_\Lambda(x)\, dx$ is the probability that the partially reflecting Brownian motion, started at the origin, is finally absorbed on the interval $(x, x + dx)$.

Note: The expression (25) can be derived directly with the help of the partially reflecting Brownian motion[3]. Indeed, consider the Brownian motion started at point $(0, \sigma\Lambda)$ with absorption probability $\sigma \ll 1$ [4]. When this motion touches the horizontal axis at some point $(x, 0)$, it will be killed with probability σ, or will be reflected into the point $(x, \sigma\Lambda)$ with probability $(1 - \sigma)$. The motion continues until being absorbed (i.e., killed) at some point. For finite σ, the distribution of hitting probabilities is given by the Cauchy density (23). It means that after each reflection we can apply this law in order to calculate the distribution of a new landing point. Using the Fourier transform and collecting the contributions after 0, 1, 2, etc. reflections, we obtain (25) in the limit $\sigma \to 0$.

The distribution $t_\Lambda(x)$ has various interesting properties, in particular:

- normalization: $\displaystyle\int_{-\infty}^{\infty} t_\Lambda(x)\; dx = 1$;
- Dirichlet limit: $t_\Lambda(x) \to \delta(x)$ when $\Lambda \to 0$;
- asymptotics at infinity: $t_\Lambda(x) \;\widetilde{x\to\infty}\; \dfrac{\Lambda}{\pi(x^2 + \Lambda^2)}$;
- asymptotics at zero: $t_\Lambda(x) \;\widetilde{x\to 0}\; -\dfrac{\ln(|x|/\Lambda) + C}{\pi\Lambda}$, where C is the Euler's constant.

[3] The authors thank Pr N.Makarov who pointed on this approach.

[4] For small $\sigma = 1 - \varepsilon$, one has $a \approx \sigma\Lambda$, see (7).

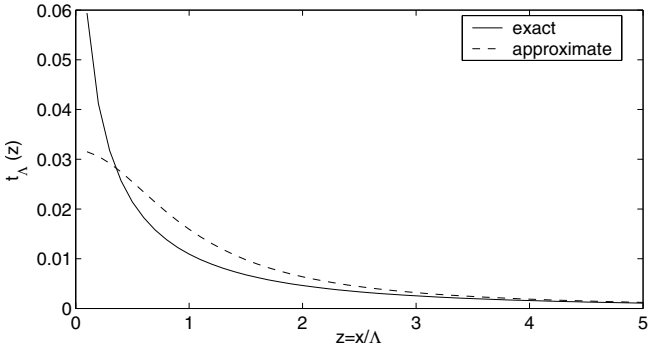

Fig. 9. The comparison of the exact distribution $t_\Lambda(x)$ with the approximate (Cauchy) distribution $\tilde{t}_\Lambda(x)$ of (26) for $\Lambda = 10$.

Using the asymptotics of $t_\Lambda(x)$ at infinity, we write the convenient form for this density:

$$t_\Lambda(x) = \eta\left(\frac{x}{\Lambda}\right)\tilde{t}_\Lambda(x) \qquad \text{with} \quad \tilde{t}_\Lambda(x) = \frac{\Lambda}{\pi(x^2 + \Lambda^2)} \quad (26)$$

where an universal function $\eta(z)$ corrects the behavior of $\tilde{t}_\Lambda(x)$ for small $z = x/\Lambda$. This function has the following properties:

- for $z \gg 1$, $\quad \eta(z) \sim 1 - 5/z^2$;
- for $z \ll 1$, $\quad \eta(z) \sim -(\ln z + C)$.

Figure 9 shows that the real distribution $t_\Lambda(x)$ is more localized around the origin. One can see that the Cauchy distribution $\dfrac{\Lambda}{\pi(x^2 + \Lambda^2)}$ gives the correct values only for $x \gg \Lambda$, i.e., for such x whose values give negligible contribution.

Note: Comparing the discrete spreading operator T_ε with the density t_Λ for the continuous case, one easily finds for the planar case:

$$(T_\varepsilon)_{0,n} \approx a\; t_\Lambda(na) \qquad (27)$$

i.e., one of them can be used to approximate the other. This relation is obtained analytically for $\Lambda \gg a$. The numerical simulations shows that this relation holds with a high accuracy even for $\Lambda \sim a$. Due to the relation (27), $\tilde{t}_\Lambda(x = na)$ is frequently used to approximate $(T_\varepsilon)_{0,n}$ for large n. As for $t_\Lambda(x)$, this approximation is convenient only for $na \gg \Lambda$.

4.3 The absorption length: the Land Surveyor Approximation

The general problem described in equations (1, 2) can also be treated through an approximate way called the *Land Surveyor Approximation (LSA)* [1,2]. The basic idea of this method consists in the following: instead of solving the problem of the Laplacian transfer across a real membrane (real geometry and finite permeability), one evaluates the Laplacian transfer across an ideal membrane (with infinite permeability) whose geometry is deduced from the initial

one through a coarse-graining procedure (or finite scale renormalization) [2].

The LSA is based on the fact that a particle, after its first hit on the membrane, will explore a region "near" this point (of course, it can go very far from the point, but the probability of this event is small). Therefore, one can suppose that there is a region (fraction of an interface) around the first hit point where the particle will be absorbed with sufficiently large probability. For a planar system, it will be shown below that the length of this region, or the *absorption perimeter length*, is approximately equal to Λ which is the physical length of this problem. Thus, each region of perimeter length Λ, independently of its geometry (which can be very complex, even pre-fractal), can be replaced by a line segment which is considered as perfectly absorbing. In mathematical language, this approximation consists in replacing the mixed boundary condition ($\nabla_n C = C/\Lambda$) on the real surface by the Dirichlet boundary condition ($C = 0$) on the new coarse-grained surface. Considerations based on Makarov's theorem [8] in $d = 2$ then permit to compute the response of a given interface from its geometry only. This method was studied numerically and experimentally for several different geometries [2].

Using the theory based on the Brownian self-transport operator, one can justify the *Land Surveyor Approximation* for the planar membrane. Indeed, one can define $\mathcal{P}_\Lambda(x)$ as the probability for a partially reflecting Brownian motion with parameter Λ starting at the origin to be finally absorbed in the interval $(-x, x)$. By definition of the kernel $t_\Lambda(x)$, $\mathcal{P}_\Lambda(x) = \int_{-x}^{x} t_\Lambda(x')\, dx'$, and this probability can be expressed as:

$$\mathcal{P}_\Lambda(x) = 1 - \frac{2}{\pi}\left[\, ci\left(\frac{x}{\Lambda}\right)\sin\left(\frac{x}{\Lambda}\right) - si\left(\frac{x}{\Lambda}\right)\cos\left(\frac{x}{\Lambda}\right)\,\right]. \tag{28}$$

Taking $x = \Lambda/2$, it comes out:

$$\mathcal{P}_\Lambda\left(\frac{\Lambda}{2}\right) \approx 0.4521. \tag{29}$$

This result allows to conclude that the region $(-\Lambda/2, \Lambda/2)$ absorbs approximately one half of the particles. Therefore Λ really plays the role of the typical absorption length along the membrane. Moreover, this important result is eventually valid for irregular geometries, see Figure 10.

Note: Using approximation (26) for $\tilde{t}_\Lambda$ to calculate the probability of particles absorbing by the region of length Λ, one easily obtains:

$$\tilde{\mathcal{P}}_\Lambda(x) = \frac{2}{\pi}\ \arctan\left(\frac{x}{\Lambda}\right).$$

For $x = \Lambda/2$, one gets an approximate value $\tilde{\mathcal{P}}_\Lambda(\Lambda/2) \approx 0.2952$ which is significantly less than the real one (29).

4.4 Numerical simulations of the spreading operator

One now investigates the properties of the discrete spreading operator T_ε from numerical simulations. The spatial distribution of the elements $(T_\varepsilon)_{i,j}$ (and $Q_{i,j}$ for comparison) with $\varepsilon \in \{0.5,\ 0.9,\ 0.99\}$ for the planar membrane is shown in Figure 11. One observes that, when ε increases, the distributions become wider in agreement with the asymptotic behavior described in (21). The spreading operator acts in an analog way as the initial Brownian self-transport operator Q but on a broader scale.

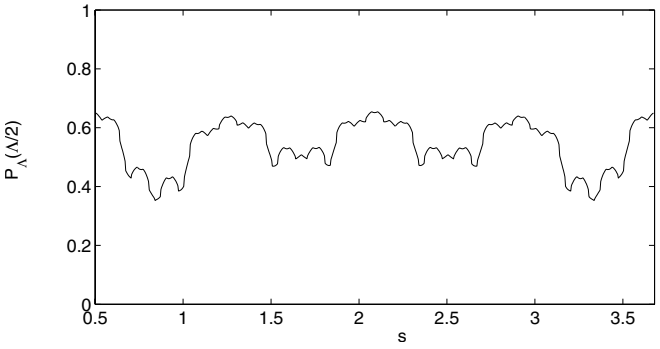

Fig. 10. Value of the probability $\mathcal{P}_\Lambda(\Lambda/2)$ as a function of the curvilinear abscissa s for a third generation of the fractal surface of Figure 2a (here, Λ is chosen equal to 1). This value represents the probability for a random walker starting at the abscissa s on the boundary to be finally absorbed in the curvilinear interval $[s - \Lambda/2, s + \Lambda/2]$ of the same boundary. One sees that this probability varies but is always of the order of 1/2, everywhere on the boundary. A random walker is thus effectively absorbed in a region of size of order Λ around its starting point.

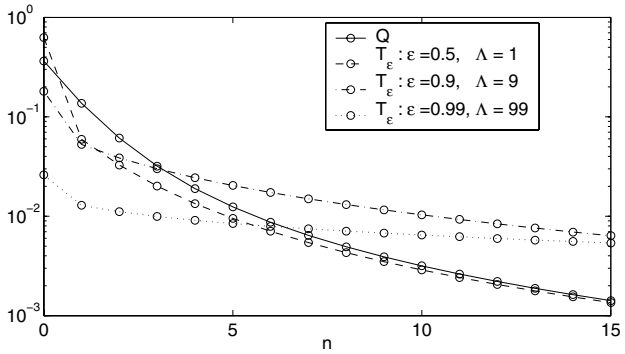

Fig. 11. The decrease of the elements $(T_\varepsilon)_{0,n}$ with increasing n for a planar membrane for several values of ε (0.5, 0.9 and 0.99).

Figure 12 gives a representative example of the dependency of the elements $Q_{i,j}$ and $(T_\varepsilon)_{i,j}$ on $|i - j|$ for the first generation of the fractal membrane of Figure 2a. One observes that Q and T_ε exhibit in general the same behavior as in planar case and that the geometries only induce relatively small variations around this common behavior.

5 Conclusion

The Brownian self-transport operator (BSO) of an interface plays a central role in understanding the Laplacian transfer across this interface (defined by the Laplace equation (1) in the bulk and the mixed boundary condition (2) on the interface). More precisely, the spectral properties of this operator determine the way the initial harmonic

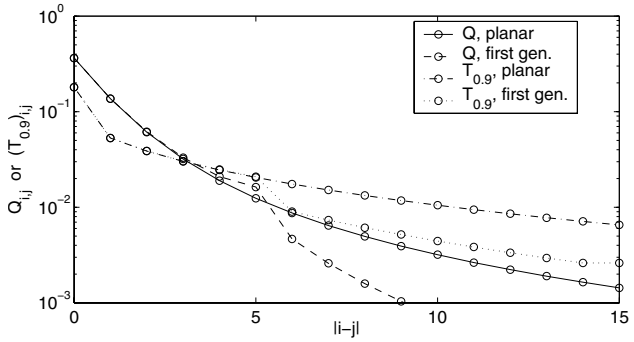

Fig. 12. The dependency of the elements $Q_{i,j}$ and $(T_\varepsilon)_{i,j}$ on $|i-j|$, with $\varepsilon = 0.9$ and fixed $i = 5$, for a planar membrane and the first generation of the fractal membrane of Figure 2a.

measure of the interface is transformed into a final current distribution on the interface. This allows to compute thereafter the macroscopic response and the impedance of the system.

As exact calculations can be carried out in the case of a flat membrane, the spectral properties of its BSO have been investigated. The eigenvalues, eigenvectors and density of states are computed exactly for a planar cyclic membrane, which is equivalent to an infinite planar membrane in the limit of a very large number of sites. The effect of a geometric irregularity of the membrane, thought as a perturbation of the flat case, is then examined through numerical simulations. It appears that the density of states $\mathcal{D}_a(q)$ is very weakly modified by the irregularity. The macroscopic response (i.e., the impedance) of the system is mainly determined by the decomposition of the harmonic measure (or *first arrival distribution*) of the interface on the eigenvectors of the BSO. This observation remains valid even for geometries of pre-fractal types. Furthermore, the number of eigenmodes that provide a significant contribution to the macroscopic response is rather small. Only one mode contributes in the case of a planar interface (the uniform eigenvector $\mathbf{1}$ which is proportional to the harmonic measure). In that case, the product $C_a^2(q)\mathcal{D}_a(q)$ is entirely concentrated at $q = 1$. For an irregular membrane, only the eigenvalues close to 1 really play a role in the Laplacian transfer. They correspond to the slowly varying eigenvectors (due to the slow variation of the harmonic measure, its scalar product with eigenvectors that have a high spatial frequency is very small).

The current distribution through a membrane with finite permeability is deduced from the first arrival distribution through a *spreading operator* T_ε. This operator depends only on the BSO and the reflection probability on the membrane. Exact expressions of this operator have been computed in the case of a planar membrane, as well as asymptotics in interesting limits ($n \gg 1$ and $\varepsilon \to 1$). Furthermore, it has been shown that in the continuous limit, this operator admits a non-trivial limit that depends also only on the geometry of the membrane and the parameter $\Lambda = D/W$. This operator is an integral operator whose kernel is also exactly computed in the case of a planar membrane. As for the BSO, asymptotic behaviors for several limits are computed.

Furthermore, thanks to this operator, one can calculate exactly the probability $\mathcal{P}_\Lambda(x)$ for a partially reflecting Brownian motion (with parameter Λ) to be absorbed in an area of radius x around its starting point. In particular, the fact that $\mathcal{P}_\Lambda(\Lambda/2) \approx 0.45$ demonstrates that the typical size of the absorption area of such a Brownian motion is Λ. Hence it justifies the *Land Surveyor Approximation* [2] as a valid approximation to solve the Laplacian problem with mixed boundary condition.

Appendix

Evaluation of the permeability in the discrete case

Here we discuss the relations between the discrete parameters (a, τ, ε) and the continuous parameters (D, W, Λ). These relations are quite general and they are valid for any dimension d of the space (lattice). The diffusion coefficient D on the hypercubic lattice is

$$D = \frac{a^2}{2d\tau}. \tag{30}$$

The semi-permeable membrane can be modelled by sites of two types: properly *surface* sites, and *absorbing* sites, Figure 13. The membrane permeability W is defined as the average flux per unit time through a planar membrane, i.e.,

$$\Phi = WC_s$$

where C_s is the concentration of particles on the surface sites.

On the other hand, one can express this flux as an elementary flux through the surface site to the absorbing site,

$$\Phi = \left(a^d C_s\right)\left(\frac{1}{a^{d-1}}\right)\left(\frac{1}{\tau_1}\right)$$

where the first factor describes the number of particles on each surface site, the second factor is inversely proportional to the area of an elementary surface a^{d-1}, and the third one is inversely proportional to the time τ_1 required to jump between surface and absorbing sites. Comparing these expressions, we find

$$W = \frac{a}{\tau_1}.$$

When a particle arrives to the surface site, it jumps to the absorbing site with *absorption probability* σ,

$$\sigma = \frac{\tau_1^{-1}}{\tau_1^{-1} + (2d\tau)^{-1}}$$

where its walking will be finished; or it goes to the neighboring bulk site with the *reflection probability* ε,

$$\varepsilon = 1 - \sigma$$

and then the walking continues as earlier. One can express W in terms of these probabilities

$$W = \frac{a}{2d\tau}\frac{1-\varepsilon}{\varepsilon}. \tag{31}$$

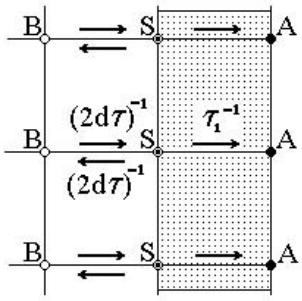

Fig. 13. The semi-permeable membrane is modelled by sites of two types: surface sites (S) and absorbing sites (A).

The substitution of the expressions (30) and (31) into the definition of Λ leads to (7),

$$\Lambda \;=\; a\,\frac{\varepsilon}{1-\varepsilon}.$$

Note: A factor $1/2d$ ($= 1/4$ in two dimensions) was missing in the original work [3].

The spread Cauchy density

Applying the spreading operator T_Λ to the Cauchy distribution (23) for the planar membrane, one obtains the *spread Cauchy density* which corresponds to the probability density of a partially reflecting Brownian motion (with parameter Λ) starting at the point (x, y) above the horizontal axis to be finally absorbed on the horizontal axis between the points $(x', 0)$ and $(x' + dx', 0)$:

$$\omega_\Lambda^{(y)}(x,x') = \frac{1}{\pi\Lambda}\int\limits_0^\infty \cos\left(\frac{k(x-x')}{\Lambda}\right)\exp\left(\frac{-ky}{\Lambda}\right)\frac{dk}{1+k}. \tag{32}$$

One can easily verify the following properties:

- normalization: $\displaystyle\int_{-\infty}^{\infty}\omega_\Lambda^{(y)}(x,x')\;dx = 1$;
- Dirichlet limit: $\displaystyle\lim_{\Lambda\to 0}\omega_\Lambda^{(y)}(x,x') = \omega_0^{(y)}(x,x')$ (i.e., the Cauchy density);
- for $y \gg \Lambda$:

$$\omega_\Lambda^{(y)}(x,x') \sim \frac{1}{\pi}\;\frac{y+\Lambda}{(x-x')^2+(y+\Lambda)^2}$$

- for $(x, y) \to (0, 0)$:

$$\omega_\Lambda^{(y)}(x,x') \sim -\frac{\ln\left(\frac{(x-x')^2+y^2}{\Lambda^2}\right)+2C}{2\pi\Lambda}.$$

Note that the third property holds even for relatively small values of y, i.e. this relation can be used as an approximation of the spread Cauchy density almost for any values of x and y (except the vicinity of the origin). An important consequence is that the partially reflecting Brownian motion starting at the point $(0, y)$ is almost equivalent to the usual Brownian motion starting at the point $(0, y + \Lambda)$. In other words, the finite permeability of the membrane effectively acts by widening (or "spreading") the arrival probability density.

References

1. B. Sapoval, Phys. Rev. Lett. **73**, 3314 (1994)
2. B. Sapoval, M. Filoche, K. Karamanos, R. Brizzi, Eur. Phys. J. B **9**, 739 (1999)
3. M. Filoche, B. Sapoval, Eur. Phys. J. B **9**, 755 (1999)
4. B. Sapoval, J.S. Andrade Jr., M. Filoche, Chem. Eng. Science V. **56**, 5011 (2001)
5. W. Feller, *An Introduction to Probability Theory and Its Applications*, Vol. II, 2nd edn (1971)
6. I.S. Gradshteyn, I.M. Ryzhik, *Table of Integrals, Series, and Products* (Academic Press, 1980)
7. F. Spitzer, *Principles of Random Walk* (Princeton, New Jersey, 1964)
8. N.G. Makarov, *On the Distortion of Boundary Sets Under Conformal Mapping*, Proc. Lond. Math. Soc. **51**, 369 (1985)
9. D.S. Grebenkov, *Propriétés de l'Opérateur d'Auto-Transport Brownien*, Rapport de stage à l'École Polytechnique, France, 2000
10. D.S. Grebenkov, *Approximate Distribution of Hitting Probabilities for a Regular Surface with Compact Support in 2D*; *Proceedings of European Summer School 2001 "Asymptotic Combinatorics with Application to Mathematical Physics", pp. 221-242, 2002*
11. T.C. Halsey, Phys. Rev. A **35**, 3512 (1987)
12. T.C. Halsey, M. Leibig, Ann. Physics **219**, 109 (1992)
13. R.C. Ball, *The Scaling of Anomalous Surface Impedance*, in *Surface Disordering, Growth, Roughening and Phase Transitions*, edited by R. Julien, J. Kertesz, P. Meakin, D. Wolf (Nova Science Publisher, 1993)